J. Condensed Matter Nucl. Sci. 37 (2023) 111–123

Research Article

A Study of Sustained Heat Generation from Pd-Ni-Zr Alloys in Hydrogen from the Viewpoint of Hydrogen Absorption

Yuya Sato, Kazumasa Oshima, Tsuyoshi Yamamoto, Masahiro Kishida*

Department of Chemical Engineering, Graduate School of Engineering, Kyushu University, Motooka 744, Nishi- ku, Fukuoka, 819-0395, Japan

Masanobu Uchimura

Research Division, Nissan Motor Co., Ltd., 1, Natsushima-cho, Yokosuka, Kanagawa, 237-8523, Japan

Abstract

In this work, the phenomenon of long-term heat generation from Pd-Ni-Zr (PNZ) alloy samples in hydrogen was investigated using differential scanning calorimetry (DSC). As a result, we succeeded in observing sustained heat generation when the PNZ sample was maintained at temperatures in the 300–500°C range. The fact that the DSC confirmed sustained heat generation over a short period of time is very significant. This is because repeated measurements over a short period of time provide more information about sustained heat generation. The relationship between sustained heat generation and hydrogen absorption behavior was examined in detail. No sustained heat generation occurred at temperatures at which the hydrogen was absorbed, while sustained heat generation occurred at the temperatures at which hydrogen was desorbed. The output of sustained heat generation decreased as the hydrogen pressure was increased. These results indicate that sustained heat generation is different from the heat of hydrogen storage. It was also found that sustained heat generation can be observed when the temperature is kept constant in the temperature range where hydrogen is being desorbed. In addition, the results of the alloy phase changes of PNZs when heat-treated in hydrogen suggested that the contribution of the alloy phase transition heat to sustained heat generation was small. Thus, it became clear that sustained heat generation in PNZs was not due to the heat of hydrogen storage, and it was suggested that the contribution of the alloy phase transition heat was small.

Keywords: Pd-Ni-Zr alloy; sustained heat generation; hydrogen absorption; DSC measurement

1. Introduction

With the global depletion of petroleum resources, expectations for renewable energy are increasing [1], [2]. However, it seems difficult to meet the overall demand of humankind with renewable energy alone. Therefore, it is important to utilize the characteristics of existing energy resources and distribute them to the right place. In the field of thermal

*Corresponding author: kishida@chem-eng.kyushu-u.ac.jp, TEL.: +81-92-802-2742, FAX.: +81-92-802-2792

© 2023 ICCF. All rights reserved. ISSN 2227-3123

energy, it has been reported in recent years that metals in hydrogen generate heat for a long period of time. Although this phenomenon does not have a large heat generation output, it is expected that the property that heat generation lasts for a long period of time will be utilized as a heat source for applications such as vehicle propulsion [3].

If heat generation is sustained for a long period of time, the total calorific value becomes enormous. It is sometimes said to be a phenomenon that is not explained by known science [4], but it is very important to clarify how much the known heat generation phenomenon contributes to this heat generation phenomenon as the first step to elucidate the mechanism. Despite this, few studies have examined the extent to which known exothermic phenomena contribute to this long-term exothermic phenomenon.

As an example of such long-term heat generation, F. Celani *et al.* reported heat generation caused by heating a CuNiMn wire. They repeatedly observed a heat generation of 2–12 W by heating an alloy wire 200 μm in diameter, 105 cm in length and 307.4 mg in weight to about 200°C under 7 bar of diluted hydrogen [5], [6]. Because the wire used is a very stable substance, it is assumed that heat generation due to the change of the sample structure during heating does not occur. Furthermore, since the components of this wire do not absorb hydrogen, the heat of hydrogen absorption in this system is expected to be very small.

Kitamura *et al.* sealed alloy powders such as Pd-Ni-Zr (PNZ) alloys or Cu-Ni-Zr (CNZ) alloys (approximately 100 g) in a vacuum-insulated container. After introducing hydrogen, the temperature was maintained at 200–300°C and the calorific value from the alloy sample was accurately measured with an oil flow calorimeter. They observed that heat generation of 3–24 W continues for several weeks from both the PNZ alloy and the CNZ alloy [7]–[9]. Iwamura *et al.* also made a similar experimental device and reported that heat generation was sustained for a long period of time from PNZ and CNZ alloys [10]. The feature of these experiments is that heat generation is observed for a long period of time from a vacuum-insulated container. Because the vacuum-insulated container can be regarded as an isolated system, the heat generation factor can be limited to the alloy and hydrogen in the system. The heat generation mechanism has not been clarified yet, but many examples of heat generation in PNZ alloys have been reported including in the proceedings of academic societies [11]–[14].

In general, there are two types of heat generated from metals in hydrogen: "heat generated from hydrogen" and "heat generated from metal". The former includes the heat of hydrogen combustion, the heat of hydrogen storage [15], [16], and the heat of hydrogen adsorption [17], [18]. Because gaseous oxygen existing in the measurement system can be easily removed by vacuum degassing, it is not necessary to consider the heat of combustion of hydrogen in the long-term heat generation phenomenon. Even if a small amount of oxygen remains, it is not possible for the combustion reaction of residual oxygen to cause heat generation that lasts for several weeks. It is also unlikely that hydrogen adsorption will occur over a long period of time. Therefore, the contribution of hydrogen storage heat should be examined in detail in the heat generation derived from hydrogen. On the other hand, the latter heat generated from metals includes the heat of metal crystallization [19], [20], the heat of phase transition of alloys [21], [22], and the heat of amorphization of metal crystals [23], [24]. These may also be involved in heat generation for a long period of time, but in this study, the effects of hydrogen storage heat were mainly examined.

Measurement of long-term heat generation is often performed using a large amount of sample material. This is because the larger the sample amount, the larger the calorific value and the better the measurement accuracy. However, using a large amount of sample has the disadvantage that it is difficult to elucidate some aspects of the phenomenon, such as the temperature distribution occurring in the sample packed bed. On the other hand, in the thermal measurement using a small amount of sample material, the measurement error becomes large, but the atmosphere around the sample layer and the sample can be regarded as uniform. Therefore, in the study of heat generation mechanism, the measurement using a small amount of sample material is more suitable.

Based on the above background, in this study, we used PNZ alloys, which are often reported to generate heat for a long time, and strictly evaluated the heat generation behavior from a small amount of PNZ sample in hydrogen using a differential scanning calorimeter. Furthermore, by comparing the hydrogen storage behavior and heat generation

Table 1. Composition of PNZ samples used in this work.

Sample	XRF analysis [mol%]			$ZrO_2/NiZr_2$	Estimated molar ratio[b)]		Estimated cont. [wt%]			
	Pd	Ni	Zr	mol ratio[a)]	$NiZr_2$/Pd	ZrO_2/Pd	Pd	Ni	$NiZr_2$	ZrO_2
PNZ(1)	4.3	31.2	64.6	1.23	4.7	5.8	5.0	7.3	53.9	33.9
PNZ(2)	4.4	31.7	63.9	1.41	4.3	6.0	5.2	8.3	50.3	36.2
PNZ(3)	4.4	31.9	63.7	1.19	4.5	5.4	5.2	7.8	54.0	33.0

a) by RIR analysis, b) assuming that Zr exists either as $NiZr_2$ or ZrO_2

behavior of PNZ samples, it was revealed that the heat of hydrogen storage does not affect the long-term exothermic phenomenon.

2. Materials and Methods

2.1. Pd-Ni-Zr (PNZ) Alloy Sample

The PNZ sample was provided by Nissan Motor Co., Ltd., and was a fine powder produced by oxidizing alloy ribbons, which are obtained by the melt spinning method, at 450°C for 60 h in air. The particle size of the PNZ powder is less than 500 micrometer. Because of the oxidation treatment, the particle surface was mainly coated with zirconium oxide, and the interior of the particle was composed of alloy phases.

The composition of the as-provided samples was analyzed using an EDX-7000 X-ray fluorescence spectrometer (Shimadzu, Japan) (Table 1). The Pd:Ni:Zr molar ratio was approximately Pd:Ni:Zr = 1:7:15. To quantify the oxide content formed by calcination, the results of X-ray diffraction (XRD) measurements as described below were analyzed using the reference intensity ratio (RIR) method [25]. The main crystal phases were $NiZr_2$ and ZrO_2, and their molar ratio was obtained as listed in Table 1. Although PNZ(1) – PNZ(3) were manufactured in different lots, their compositions were almost the same.

2.2. Crystal Phase of PNZ

The XRD pattern of the PNZ sample was obtained using an Ultima IV diffractometer (Rigaku, Japan) using Cu–Kα radiation ($\lambda = 0.15418$ nm) in the scattering angle (2θ) range of 20–80°. The crystalline phase of the sample was identified using the Joint Committee on Powder Diffraction Standards (JCPDS) database. The content of the main metal alloy and ZrO_2 was estimated using the RIR method [25].

2.3. H_2 Absorption/Desorption Behavior

Hydrogen absorption and desorption were characterized by the temperature-programmed reaction (TPR) method using a BELCAT-B catalyst characterization analyzer (Microtrac), equipped with a quadrupole mass spectrometer (QMS). A sample of 100 mg mass was placed in a sample tube and heated at 5°C/min while distributing 4.89 vol% hydrogen gas (argon balance) under atmospheric pressure, and the change in the hydrogen concentration of the outlet gas was analyzed by QMS. The temperature range was 30–800°C. Measurements were also performed as required by holding the sample at a predetermined temperature.

2.4. Exothermic/Endothermic Behavior

The exothermic and endothermic behaviors of the samples were evaluated by differential scanning calorimetry (DSC) using a PT-1600H calorimeter (Linseis, Germany) with a controllable gas atmosphere. The apparatus can be set up with

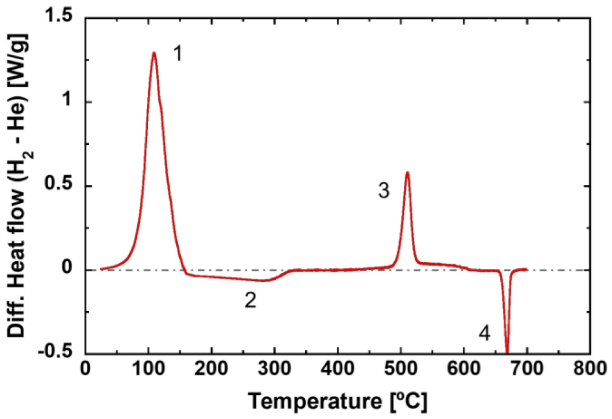

Figure 1. DSC thermogram of the PNZ (1) sample at elevated temperatures.

two containers, one for the measurement sample and the other for the reference sample, and the baseline measurement was performed with both containers being empty. Thereafter, with the reference sample container empty, a sample of 25–100 mg was loaded into the measurement sample container, whereafter it was evacuated until the pressure became lower than 10^{-3} Pa. Subsequently, high-purity hydrogen (99.9999 vol%) was flowed at a rate of 70 mL/min under atmospheric pressure to begin the measurement. However, pressures up to 2.0 x 10^5 Pa were used in the experiments to examine pressure dependence. During measurement, the sample was elevated to a predetermined temperature at 5°C/min and maintained for 4 h. Following this measurement, the distribution gas was switched to helium, and the temperature was cooled to lower than 30°C. Thereupon, thermal measurements were performed at an identical temperature profile in helium flow. The measurements in hydrogen and helium were repeated as necessary.

3. Results and Discussion

In previous reports, long-term exothermic phenomena have been observed under conditions where the temperature is maintained at a fixed level. However, we first examined the heat generation behavior from PNZ samples while increasing the temperature. Figure 1 shows the DSC output when the PNZ (1) sample was heated to 800°C (5°C / min) in pure hydrogen. Exothermic peaks were observed near 100°C and 520°C, and endothermic peaks were observed near 660°C. As described below, these exothermic and endothermic peaks were attributed to hydrogen absorption and desorption, respectively, and no anomalous heat generation was observed. In the report by Kitamura *et al*., long-term heat generation of up to 10 W was observed using a PNZ sample of about 100 g, but even if a similar heat generation phenomenon occurred in Fig. 1, it may be difficult to observe it as an exothermic peak during temperature rise.

Figure 2 shows the DSC measurement results of Ni metal powder that does not generate any heat in hydrogen. After raising the temperature from room temperature to a predetermined temperature at 5°C/min, the measurement was carried out continuously at that temperature in H_2 flow and He flow, in that order. When the temperature was kept at 350–450°C, the heat flow while the temperature was held steady was almost the same in H_2 and He. Ni metals should occlude almost no hydrogen in this temperature range and generate no heat. In this way, it was shown that the heat flow of this device in H_2 and He was the same in the absence of heat generation in H_2 from the sample.

Figure 3 shows the results of DSC measurement of PNZ (1) – PNZ (3) under the same conditions as in Fig. 2.

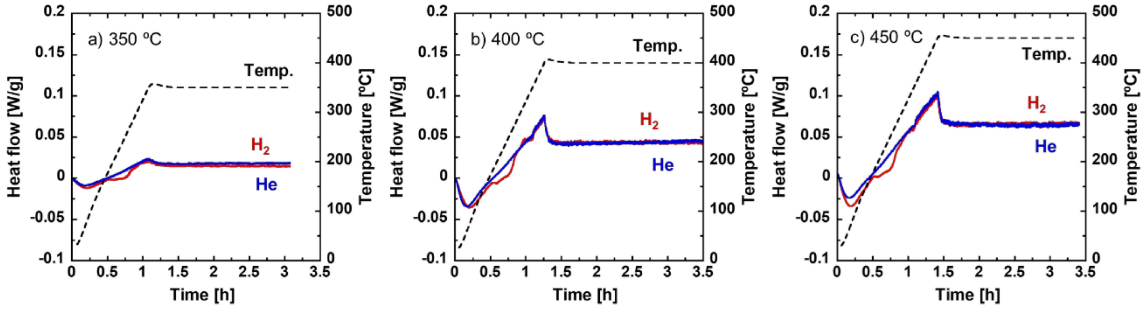

Figure 2. DSC thermograms of Ni powder in H_2 and He flow.

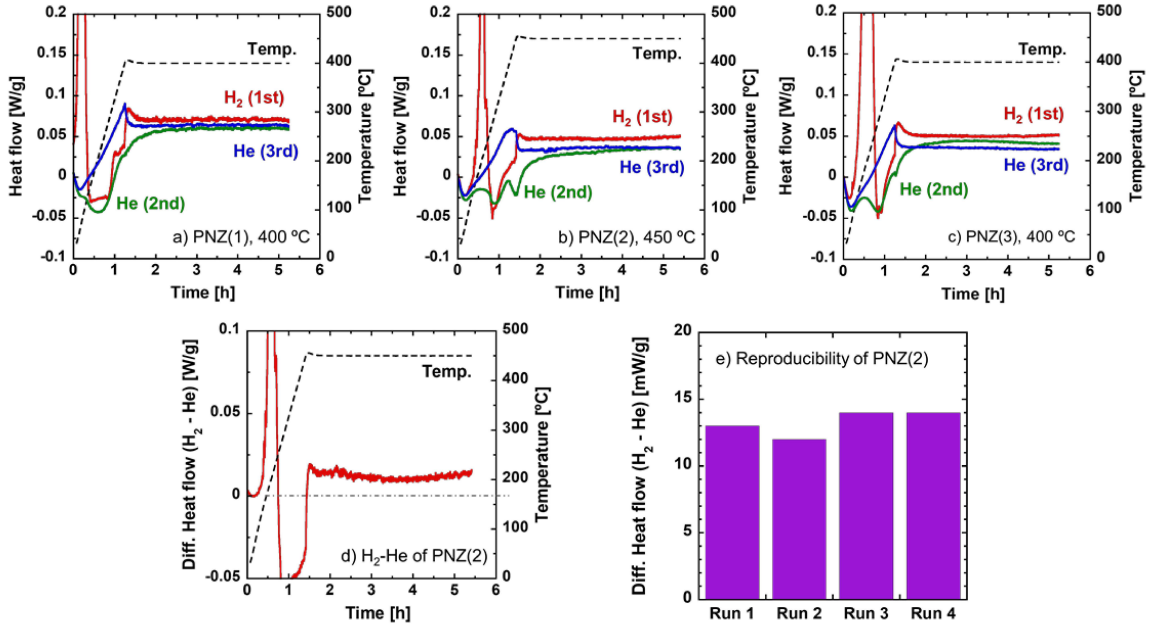

Figure 3. DSC thermograms of a) PNZ (1), b), d), and e) PNZ (2), and c) PNZ (3) in H_2 and He flow.

In the measurements in H_2, a large exothermic peak was observed below 200°C, and a small endothermic peak above 200°C for all the samples of PNZ (1)–(3) during the temperature increase process. As described below, these exothermic and endothermic peaks were attributed to hydrogen absorption and desorption, respectively. Focusing on the heat flow during a fixed temperature, the heat flow in H_2 exceeded the heat flow in He for all the samples of PNZ (1) – (3). The difference was 7–17 mW/g, which varied depending on the lot, but it is clear that there is a difference in heat flow between H_2 and He. The heat flow difference between H_2 (1st) and He (3rd) of PNZ (2) is plotted in Fig. 3 d), and the heat flow difference of 13 mW/g was continuously observed when the temperature was

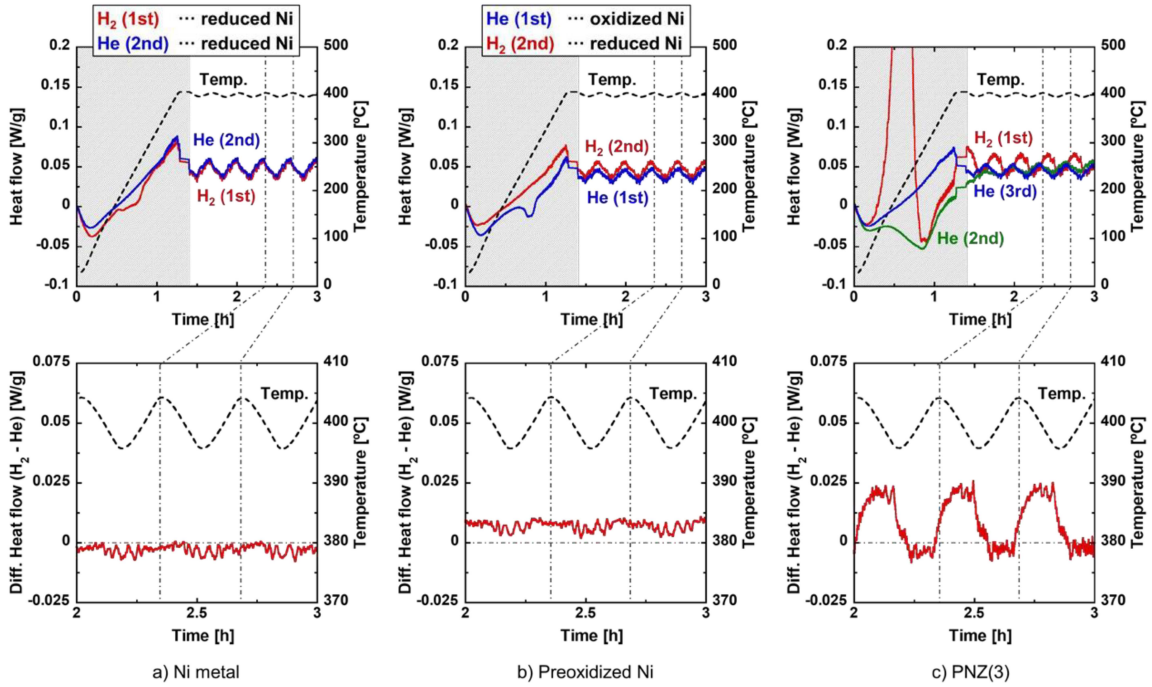

Figure 4. DSC thermograms of the a) Ni, b) pre-oxidized Ni, c) PNZ (3) when the temperature was periodically varied.

maintained. When the same experiment was repeated 4 times using PNZ (2), the heat flow difference when held at 450°C was 13 ± 1 mW/g, with good reproducibility (Fig. 3 e).

In general, differences in DSC heat flow when holding a fixed temperature are often attributed to differences in heat capacity or thermal conductivity of the samples. In the measurement in Fig. 3, the same sample is measured continuously in hydrogen and helium, but the heat capacity or thermal conductivity may change as the sample absorbs hydrogen. In order to determine whether the difference in heat flow during a fixed temperature is due to heat generated from the PNZ sample, a DSC measurement was conducted in which the temperature was periodically varied (400 ± 5°C at 5°C / min) (Figure 4). The upper figures of Fig. 4 show the variation of heat flow in H_2 (red line) and He (blue line) with the temperature change (dashed line). The lower figures in Fig. 4 show the result of subtracting the heat flow in He from the heat flow in H_2 (red line) in the process of periodically changing the temperature in the upper figures, along with the temperature change (dashed line). For the Ni metal powder measurement in Fig. 4 a), there was no difference at all between the heat flow in H_2 and He in the process of periodic temperature change. In Fig. 4 b), pre-oxidized Ni was measured in He flow and H_2 flow, in that order. In this case, the heat flow between H_2 and He was different in the process of periodic temperature change. The heat capacity or thermal conductivity was different in both measurements due to the different oxidation state of Ni. The difference is considered to have appeared as a difference in the heat flow of DSC. The lower figure of Fig. 4 b) shows that the difference between the heat flow in H_2 and He was constant even when the temperature was periodically changed. In addition, the phase of the heat flow change coincided with the phase of the temperature change. When the heat capacity and thermal conductivity of the sample differ in hydrogen and helium, the difference in heat flow appears during the periodic temperature change

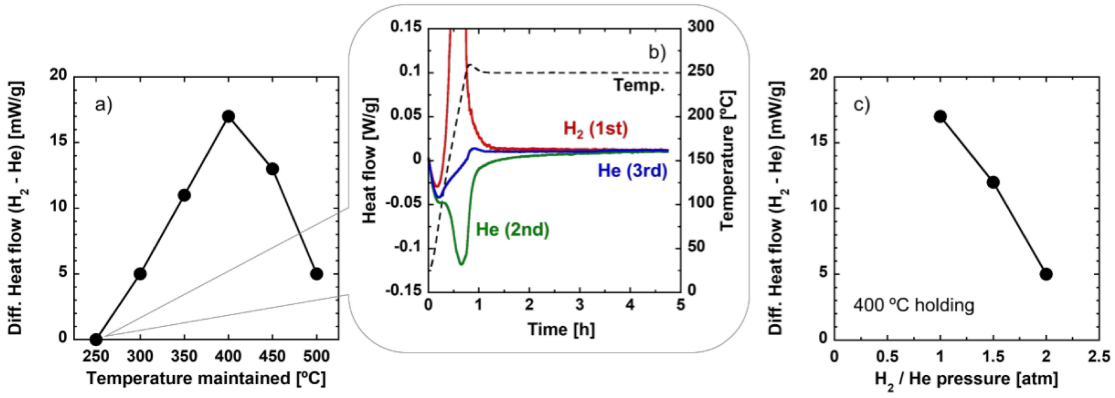

Figure 5. Effects of maintained temperature and pressure on differences between the DSC thermograms of PNZ (3) in H_2 and He.

process, but the difference is independent of the periodic temperature change. On the other hand, in the PNZ(3) in Fig. 4 c), the heat flow in H_2 exceeded that in He during the periodic temperature change process, as in the fixed temperature experiment in Fig. 3. As can be seen from the lower figure in Fig. 4 c), the difference between the heat flow in H_2 and He changed between 0–25 mW/g with periodic temperature change. The maximum heat flow difference of 25 mW/g was larger than the heat flow difference of 17 mW/g in Fig. 3 c). The hydrogen storage amount changes with a temperature change of $\pm$ 5°C, but the amount of change must be smaller than the difference in hydrogen storage in H_2 (1st) and He (3rd) in Fig. 3 c). In addition, the phase of the heat flow difference change was shifted by about 1/4 period with respect to the phase of the temperature change. Therefore, it is clear that the PNZ samples generate heat in H_2. The fact that no decay of heat flow was observed during the 4-hour temperature holding period in Fig. 3 indicates that PNZ has a property of long-term persistence in its heat generation. Although these properties of PNZ have already been reported, it is significant that this long-term sustained heat generation was confirmed by short-time measurements using DSC. The reason for this is that by measuring under different conditions, much more information about sustained heat generation can be obtained.

Next, we measured the heat flow of sustained heat generation, that is, the difference in heat flow in hydrogen and in helium, under different conditions. Figure 5 shows a) the fixed temperature dependence and c) the H_2 partial pressure dependence of the heat flow of sustained heat generation from PNZ sample during a fixed temperature. In Fig. 5 a), the heat flow of sustained heat generation began to appear at temperatures higher than 250°C, became maximum at 400°C, and decreased at temperatures higher than that. As shown in Fig. 5 b), sustained heat generation was not observed when the temperature was maintained at 250°C, where the heat generation was not completed during the temperature increase. In Fig. 5 c), as the H_2 partial pressure increased from 1 atm to 3 atm, sustained heat flow became smaller. It is noteworthy that the higher the H_2 pressure, the larger the hydrogen storage should be, but sustained heat generation is smaller. These behaviors will be discussed later.

Since the PNZ sample was found to generate heat continuously in hydrogen, the hydrogen absorption behavior of the PNZ sample was examined by the TPR method using QMS. Figure 6 shows the change in the QMS intensity of hydrogen (m / z = 2) when the temperature is raised to 800°C at 5°C / min and the temperature is maintained at 800°C. In the blank experiment measured without a sample, there was no change in the QMS intensity even when the temperature rise was stopped at 800°C. The baseline (dashed line in Fig. 6) was determined from the curve when the temperature was maintained. The QMS intensity of water (m/z = 18) was also measured during this measurement, but no water formation was observed in any of the samples. Therefore, the change in QMS intensity of hydrogen is due to

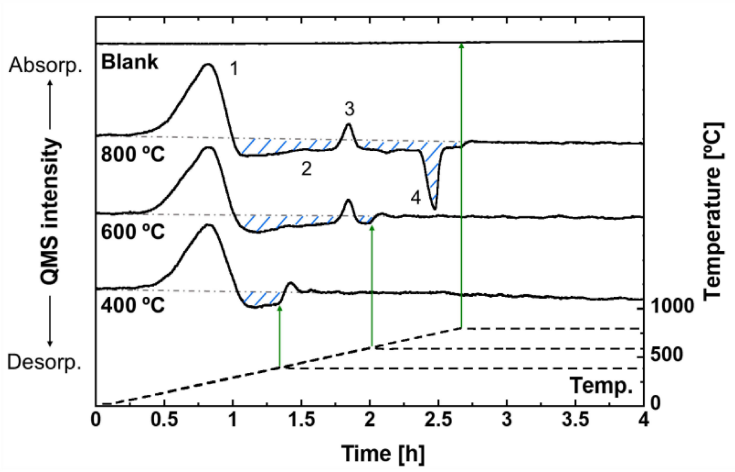

Figure 6. QMS spectra of H_2 (m/z = 2) when the temperature was increased and maintained using 4.89% H_2.

the absorption and desorption of hydrogen by PNZ. Focusing on the change during temperature rise in Fig. 6, a peak of hydrogen absorption (Peak 1) was observed near 230°C. As shown in Table 1, the main alloy phase of the PNZ samples is $NiZr_2$. Aoki *et al*. obtained a hydrogen storage isotherm of $NiZr_2$ at 200°C [26], which is consistent with the fact that the PNZ (1) sample absorbed hydrogen in this temperature range. The amount of hydrogen absorption at Peak 1 was 1.5 mol/mol-$NiZr_2$. This value is smaller than the previous reports (2.0 mol/mol-$NiZr_2$) [27] in the Ni-Zr alloy, but the main reason for this is that the absorption equilibrium has not been reached. From 300°C to 800°C in Fig. 6 (Range 2), hydrogen desorption was observed, which is evident from the step-like change in QMS intensity when switching from increasing temperature to a fixed temperature (400, 600, 800°C). The slow desorption of hydrogen at Range 2 may be due to the slow rate of mass transfer within the alloy. Such slow hydrogen desorption by heating in hydrogen has also been reported in Fe_2Gd [28]. As the temperature continued to rise, a hydrogen absorption peak (Peak 3) was observed at 550°C and a hydrogen desorption peak (Peak 4) was observed near 740°C. These hydrogen absorption and desorption correspond to disproportionation of the $NiZr_2$ phase and hydrogen desorption from the disproportionation products, respectively. However, as shown in Fig. 5 a), little sustained heat generation was observed in the temperature range above 500°C. This suggests that the disproportionation of the $NiZr_2$ phase in hydrogen has little effect on sustained heat generation from PNZ. Here, we consider the relationship between sustained heat generation and hydrogen storage heat. sustained heat generation occurs only in hydrogen, so the phenomenon must require hydrogen. However, as shown in Fig. 5 b), sustained heat generation did not occur even when the temperature was held constant in the range at which hydrogen is absorbed. On the other hand, Figs. 5 a) and 6 show that hydrogen desorption occurs in the 300–500°C range where sustained heat generation occurs. Hydrogen desorption is also confirmed by the endotherm observed during the temperature rising process in Fig. 3 d). These results indicate that sustained heat generation in PNZ samples is different from the heat of hydrogen storage and that sustained heat generation occurs during hydrogen desorption. To confirm this, DSC measurement was performed by raising the temperature to 400°C while supplying hydrogen, and switching the gas to helium at the start of holding the temperature at a fixed level (Figure. 7). The vertical axis in Fig. 7 shows the difference from the heat flow measured in helium from the beginning with the same temperature profile. When the gas was switched to helium at 400°C, the heat flow was disturbed, but heat generation was observed for about 2 h thereafter. The absorbed hydrogen should be

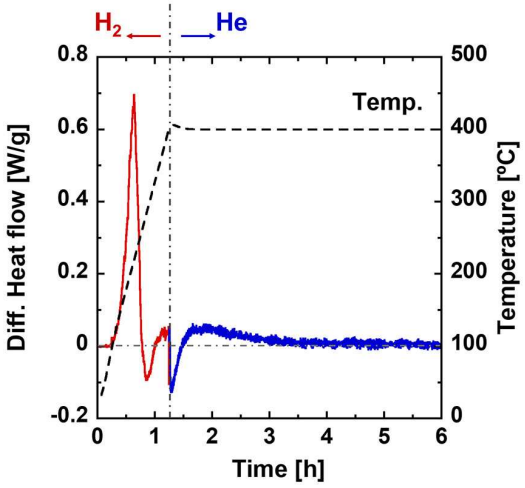

Figure 7. DSC output of PNZ (3) when the temperature was raised in H_2 and then maintained at 400°C in He.

quickly desorbed at 400°C in helium, but nevertheless heat generation occurred for about 2 h. This indicates that the heat generated from the PNZ when the temperature is maintained is not due to the heat of hydrogen storage.

If we assume sustained heat generation occurs during hydrogen desorption, that would explain why heat generation decreases as the hydrogen pressure increases. Furthermore, it can be understood that if sustained heat is generated during hydrogen desorption, it was not observed by DSC measurement while raising the temperature. This is because the endothermic process due to hydrogen desorption hides the minute heat generation. When switching from a rising temperature to a fixed temperature in the QMS measurement shown in Fig. 6, the hydrogen desorption that had occurred up to that point stopped immediately. Thus, it can be said that the hidden sustained heat generation became apparent by maintaining the temperature at a fixed level.

The phenomenon of heat generation in a sample during hydrogen desorption can also be explained by the following model. If a more stable hydrogen storage phase coexists apart from the hydrogen storage phase in which desorption is observed and hydrogen transfer occurs between those phases, that is, small heat absorption (desorption) and large heat generation (absorption) occur. If they occur together, as a result, heat generation may be observed during hydrogen desorption. However, such a model cannot explain that the higher the hydrogen pressure, the smaller the heat flow due to sustained heat generation. In summary, sustained heat generation observed in the PNZ samples at 300–500°C is different from the heat of hydrogen storage. It was also found that sustained heat generation occurred during the desorption of hydrogen.

Finally, the contribution of the phase transition in PNZ samples to sustained heat generation was examined. Figure 8 shows the XRD measurement results of PNZ samples heated for 4 h in a) pure hydrogen and b) diluted hydrogen (4.89 vol%). In the XRD pattern of the as-provided sample, a peak of $NiZr_2$ alloy and a peak of monoclinic ZrO_2 were observed. Because this PNZ sample is provided after calcining at 450°C in air, the as-provided sample surface is oxidized. It was shown that the surface oxide phase is mainly ZrO_2. In a Ni-Zr alloy (Ni:Zr=7:15) containing no Pd, $NiZr_2$ becomes the main alloy phase [29], and so it is reasonable that $NiZr_2$ is the main alloy phase even in this sample containing a small amount of Pd. When treated with pure hydrogen at 200°C as shown in Fig. 8 a), the $NiZr_2$ peak disappeared and new peaks of 33.5, 37.2, and 41.9 degrees appeared. Their peaks were observed even after 400°C treatment. Similar changes in these peaks were observed in dilute hydrogen in Fig. 8 b). The changes are due

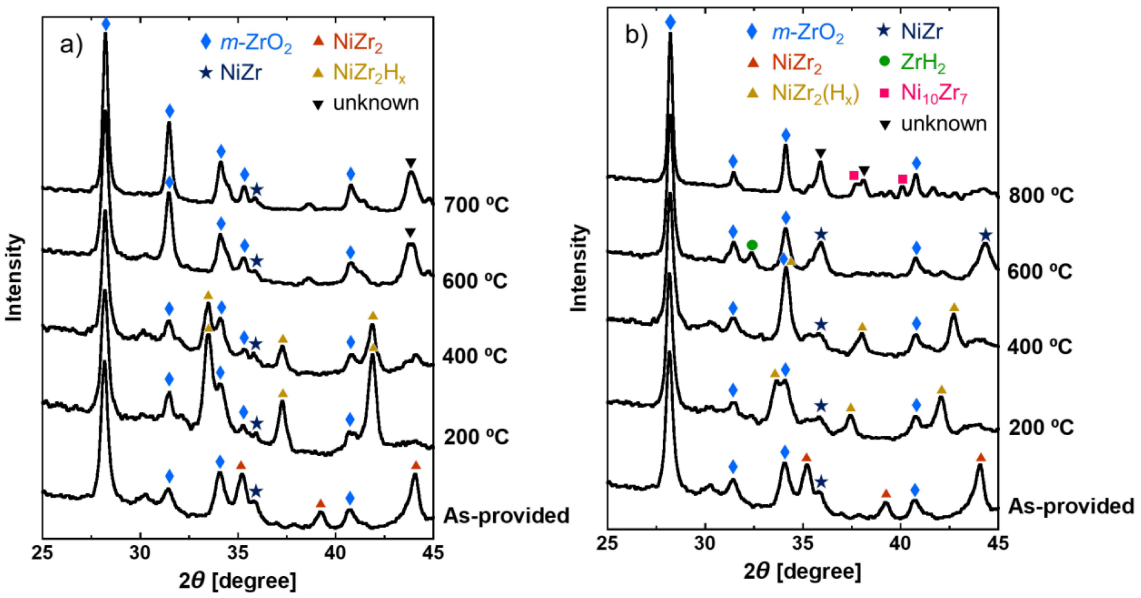

Figure 8. XRD patterns of PNZ (1) heated in a) pure H_2 and b) 4.89% H_2 at predetermined temperature for 4 hours.

to hydrogen absorption, since the PNZ sample absorbs hydrogen at 200°C (Fig. 6). It has been reported that $NiZr_2$ absorbs hydrogen and undergoes a disproportionation reaction to form NiZr hydride and Zr hydride [30]–[32], while others have reported the formation of $NiZr_2$ hydride without disproportionation at room temperature [27]. Because the peak positions of $NiZr_2$ hydride and NiZr hydride are similar, it is difficult to distinguish them. In any case, XRD measurements showed that the phase transition of the alloy phase of PNZ was barely observed at around 400°C, where sustained heat generation was observed.

The results of repeated measurements in hydrogen or helium are shown in Figure 9. As in Fig. 3, sustained heat generation was observed during the first measurement in H_2 (1st). In subsequent measurements in helium, the heat flow decreased, but the heat flow in H_2 (5th) for the fifth measurement matched the heat flow in H_2 (1st). Since the disproportionation reaction of $NiZr_2$ phase can proceed when hydrogen is absorbed, if the heat of disproportionation reaction is observed, the heat flow of the 5th measurement should be lower than that of the 1st measurement. However, the fact that no decrease was observed in the result in H_2 (5th) suggests that the heat of disproportionation reaction has little effect on sustained heat generation. These results alone do not indicate that the alloy phase transition heat does not contribute to sustained heat generation at all, but at least the contribution of the alloy phase transition heat to sustained heat generation is considered to be small.

4. Conclusion

In this work, the phenomenon of long-term heat generation from Pd-Ni-Zr (PNZ) alloy samples in hydrogen was investigated using differential scanning calorimetry (DSC). As a result, we succeeded in observing sustained heat generation when the PNZ sample was maintained at temperatures in the 300–500°C range. Although such long-term heat generation of PNZs has already been reported, the fact that sustained heat generation was observed in a short time

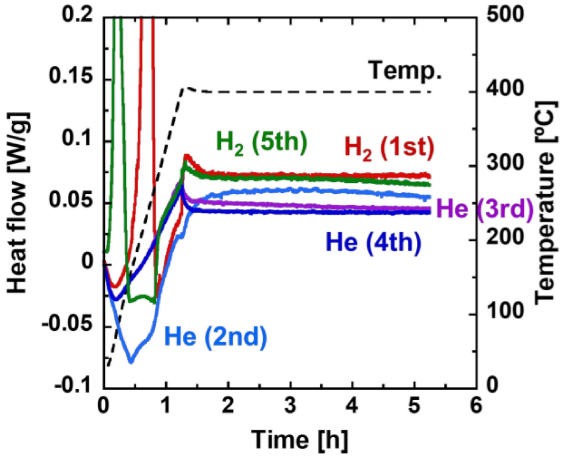

Figure 9. Repeated DSC measurements of PNZ(2) samples. Measurement sequence: H_2 (1st) - He (2nd) - He (3rd) - He (4th) - H_2 (5th).

by DSC is very significant. Short-time measurements can provide more information on sustained heat generation, since many measurements can be performed under different conditions. In fact, this work provided a variety of information, including the temperature range over which sustained heat generation occurs and the dependence on hydrogen pressure.

The relationship between sustained heat generation and hydrogen absorption behavior was examined in detail. No sustained heat generation occurred at the temperature at which hydrogen was absorbed, while sustained heat generation occurred at the temperature at which hydrogen was desorbed. The output of sustained heat generation decreased as the hydrogen pressure was increased. These results indicate that sustained heat generation is different from the heat of hydrogen storage. It was also found that sustained heat generation can be observed when the temperature is kept constant in the temperature range where hydrogen is being desorbed. Since sustained heat generation is masked by endotherm due to hydrogen desorption, it is not observed unless the temperature is maintained at a fixed level.

In addition, the change in the alloy phase of PNZ when heat-treated in hydrogen was examined, and it was found that the main alloy phase of PNZ is $NiZr_2$, and that $NiZr_2$ absorbs and desorbs hydrogen. However, the disproportionation reaction that occurs during hydrogen absorption in $NiZr_2$ was not observed in the temperature range where sustained heat generation was observed. These results and the repeated DSC measurements suggest that the contribution of the alloy phase transition heat to sustained heat generation is small.

Thus, it became clear that sustained heat generation in PNZs was not due to the heat of hydrogen storage, and it was suggested that the contribution of the alloy phase transition heat was small. Although the mechanism of sustained heat generation remains to be elucidated, the possibility of cold fusion remains.

5. Acknowledgements

The authors would like to thank Nissan Motor Co., Ltd. for providing us with metal-alloy samples and for funding this research work. We are also grateful to Tosoh Corporation for research funding.

References

[1] J. Lian, Y. Zhang, C. Ma, Y. Yang, E. Chaima, A review on recent sizing methodologies of hybrid renewable energy systems, *Energy Convers Manage* **199** (2019) 112027. DOI: 10.1016/j.enconman.2019.112027.

[2] M. Hirscher, V.A. Yartys, M. Baricco, J. Bellosta Von Colbe, D. Blanchard, R.C. Bowman, *et al*, Materials for hydrogen-based energy storage – past, recent progress and future outlook, *J Alloys Compd* **827** (2020) 153548. DOI: 10.1016/j.jallcom.2019.153548.

[3] Z. Zhang, X. Zhang, W. Chen, Y. Rasim, W. Salman, H. Pan, *et al*, A high-efficiency energy regenerative shock absorber using supercapacitors for renewable energy applications in range extended electric vehicle, *Appl Energy* **178** (2016) 177–188. DOI: 10.1016/j.apenergy.2016.06.054.

[4] S. Focardi, R. Habel, F. Piantelli, Anomalous heat product in Ni-H systems, *Il Nuovo Cimento A* **107**(1) (1994) 163–167. DOI: 10.1007/bf02813080.

[5] F. Celani, A. Spallone, B. Ortenzi, S. Pella, E. Purchi, F. Santandrea, *et al*, Observation of macroscopic current and thermal anomalies, at high temperature, by hetero-structures on thin and long Constantan wires under H_2 gas, *J Condensed Matter Nucl Sci* **19** (2016) 29–45.

[6] F. Celani, C. Lorenzetti, G. Vassallo, E. Purchi, S. Fiorilla, S. Cupellini, *et al*, Progress Toward an Understanding of LENR–AHE Effects in Coated Constantan Wires in D2 Atmosphere: DC/AC Voltage Stimulation, *J Condensed Matter Nucl Sci* **33** (2020) 1–28.

[7] A. Kitamura, A. Takahashi, R. Seto, Y. Fujita, A. Taniike, Y. Furuyama, Brief summary of latest experimental results with a mass-flow calorimetry system for anomalous heat effect of nano-composite metals under D(H)- gas charging, *Curr Sci* **108**(4) (2015) 589–593.

[8] A. Kitamura, A. Takahashi, K. Takahashi, R. Seto, Y. Matsuda. Collaborative Examination on Anomalous Heat Effect Using Nickel-based Binary Nanocomposites Supported by Zirconia. *J Condensed Matter Nucl Sci* **24** (2017) 202–213.

[9] A. Kitamura, A. Takahashi, K. Takahashi, R. Seto, T. Hatano, Y. Iwamura, *et al*, Excess heat evolution from nanocomposite samples under exposure to hydrogen isotope gases, *Int J Hydrogen Energy* **43**(33) (2018) 16187–16200. DOI: 10.1016/j.ijhydene.2018.06.187.

[10] Y. Iwamura, T. Itoh, J. Kasagi, A. Kitamura, A. Takahashi, K. Takahashi, Replication Experiments at Tohoku University on Anomalous Heat Generation Using Nickel-based Binary Nanocomposites and Hydrogen Isotope Gas, *J Condensed Matter Nucl Sci* **24** (2017) 191–201.

[11] A. Kitamura, E.F. Marano, A. Takahashi, R. Seto, T. Yokose, A. Taniike, *et al*, Heat evolution from zirconia- supported Ni-based nano-composite samples under exposure to hydrogen isotope gas, in: K. Tsuchiya (Ed.), *Proceedings of 16th Meeting of Japan CF-Research Society (JCF16)* (Kyoto, 2015) pp. 1–16.

[12] A. Kitamura, A. Takahashi, K. Takahashi, R. Seto, T. Hatano, Y. Iwamura, *et al*, Comparison of excess heat evolution from zirconia-supported Pd-Ni nanocomposite samples with different Pd/Ni ratio under exposure to hydrogen isotope gases, in: Y. Iwamura (Ed.), *Proceedings of 18th Meeting of Japan CF-Research Society (JCF18)* (Sendai, 2017) pp. 14–31.

[13] A. Takahashi, T. Yokose, Y. Mori, A. Taniike, Y. Furuyama, H. Ido, *et al*, Enhancement of Excess Thermal Power in Interaction of Nano-Metal and H(D)-Gas, in: M. Kishida (Ed.), *Proceedings of 20th Meeting of Japan CF-Research Society (JCF20)* (Hakata, 2019) pp. 9–27

[14] A. Takahashi, H. Ido, A. Hattori, R. Seto, A. Kamei, J. Hachisuka, *et al*, Latest Progress in Research on AHE and Circumstantial Nuclear Evidence by Interaction of Nano-Metal and H(D)-Gas. *J Condensed Matter Nucl Sci* **33** (2020) 14–32.

[15] E. Akiba. Fundamentals. in: K. Sasaki, H.-W. Li, A. Hayashi, J. Yamabe, T. Ogura, S.M. Lyth (Eds), *Hydrogen Energy Engineering: Springer Japan* (2016) pp. 177–190. DOI: 10.1007/978-4-431-56042-5_13.

[16] E. Wicke, H. Brodowsky, H. Züchner. Hydrogen in palladium and palladium alloys, in: G. Alefeld, J. Völkl J (Eds). *Hydrogen in Metals II: Springer Berlin Heidelberg* (1978) pp. 73–155. DOI: 10.1007/3-540-08883- 0_19.

[17] V.P. Londhe, N.M. Gupta, Adsorption and Microcalorimetric Measurements on the Interaction of CO and H_2 with Polycrystalline Ru and Ru/TiO2 Catalyst, *J Catal* **169**(2) (1997) 415–422. DOI: 10.1006/jcat.1997.1717.

[18] H. Yang, J.L. Whitten, Dissociative adsorption of H_2 on Ni(111), *J Chem Phys* **98**(6) (1993) 5039–5049. DOI: 10.1063/1.464958.

[19] U. Köster, U. Herold. Crystallization of metallic glasses, in: H.-J. Güntherodt, H. Beck, (Eds). *Glassy Metals I: Springer Berlin Heidelberg* 1981. pp. 225–259. DOI: 10.1007/3540104402_10.

[20] T. Ichitsubo, E. Matsubara, H. Numakura, K. Tanaka, N. Nishiyama, R. Tarumi, Glass-liquid transition in a less-stable metallic glass. *Phys Rev B* **72**(5) (2005). DOI: 10.1103/PhysRevB.72.052201.

[21] L. Battezzati, M. Belotti, V. Brunella, Calorimetry of ordering and disordering in AuCu alloys, *Scr Mater* **44**(12) (2001) 2759–2764. DOI: 10.1016/S1359-6462(01)00961-7.
[22] N. Terashita, E. Akiba, Hydrogenation Properties of CaMg2 Based Alloys, *Mater Trans* **45**(8) (2004) 2594–2597. DOI: 10.2320/matertrans.45.2594.
[23] K. Aoki. Amorphous phase formation by hydrogen absorption. *Mater Sci Eng A* **304–306** (2001) 45–53. DOI: 10.1016/S0921-5093(00)01432-5.
[24] X. G. Li, A. Chiba, K. Aoki, T. Masumoto. Differential thermal analysis of hydrogen-induced amorphization in C15 Laves compounds RFe2. *Intermetallics* **5**(5) (1997) 387–391. DOI: 10.1016/S0966- 9795(97)00009-5.
[25] C.R. Hubbard, R.L. Snyder. RIR - Measurement and Use in Quantitative XRD. Powder Diffr **3**(2) (1988) 74–77. DOI: 10.1017/S0885715600013257.
[26] K. Aoki, M. Kamachi, T. Masumoto. Thermodynamics of hydrogen absorption in amorphous ZrNi alloys. *J Non-Cryst Solids* **61–62** (1984) 679–684. DOI: 10.1016/0022-3093(84)90624-0.
[27] M. Hara, R. Hayakawa, Y. Kaneko, K. Watanabe. Hydrogen-induced disproportionation of Zr2M (M=Fe, Co, Ni) and reproportionation. *J Alloy Compd* **352** (2003) 218–225. DOI: 10.1016/s0925-8388(02)01169-6
[28] K. Aoki, T. Matsumoto. Hydrogen-induced amorphization of intermetallics. *J Alloy Compd* **231** (1995) 20–28. DOI: 10.1016/0925-8388(95)01832-8
[29] N. Wang, C. Li, Z. Du, F. Wang. Experimental study and thermodynamic re-assessment of the Ni-Zr system. *Calphad* **31**(4) (2007) 413–421. DOI: 10.1016/j.calphad.2007.07.001.
[30] M.J. Trzeciak, D.F. Dilthey, M.W. Mallett, Battelle Memorial Institute [Report, p. BMI-1112];1956.
[31] H. Shaaban, E. Karakish, A. Shaaban, S. Isaack. Thermal hydriding of some Ni-based intermetallic compounds. *Int J Hydrogen Energy* **18**(7) (1993) 571–574. DOI: 10.1016/0360-3199(93)90177-c.
[32] K. Aoki, T. Matsumoto. Structural Change and Crystallization Process of As-quenched or Hydrogenated Amorphous Zr-Ni Alloys during Heating in H_2 or Ar Atmosphere. *J Jpn Inst Met* **49**(1) (1985) 89–96. DOI: 10.2320/jinstmet1952.49.1_89